STUDIA UNIVERSITATIS BABES-BOLYAI, CHEMIA, LIV, 1, 2009

Dedicated to Professor Liviu Literat, at his 80th anniversary

PROCAINE EFFECTS ON SURFACE TOPOGRAPHY OF SPREAD DIPALMITOYL PHOSPHATIDYLCHOLINE MONOLAYERS

PETRE T. FRANGOPOL[a], D. ALLAN CADENHEAD[b], MARIA TOMOAIA-COTIŞEL[c*] AND AURORA MOCANU[c]

ABSTRACT. The surface topography of dipalmitoyl phosphatidylcholine (DPPC) monolayers, spread at the air/water interface, in the absence and the presence of procaine, has been investigated by self-assembly Langmuir-Blodgett (LB) technique and atomic force microscopy (AFM), operating in tapping mode. The LB monolayers were transferred on mica, at a controlled surface pressure, characteristic for the liquid expanded to liquid condensed phase transition of pure DPPC monolayers. Our data indicate that procaine penetrates into and specifically interacts with DPPC monolayers stabilizing the phospholipid membrane interface.

Keywords: *DPPC, procaine, monolayers, AFM, LBT, phase transition*

INTRODUCTION

Changes in physical and chemical properties of lipid membranes due to the distribution of local anesthetics within these membranes are of a major importance [1-4] for understanding the molecular mechanism of anesthesia. In spite of numerous investigations, the molecular mechanism of anesthesia and the involved interfacial phenomena in anesthetics action are still not well understood [5]. As a first step, the anesthetics action presumes that the anesthetic molecules modify the lipid membrane structure and thus, they change the biological membrane properties [5].

[a] *Institutul Național de Fizică şi Inginerie Nucleară Horia Hulubei, Str. Atomiştilor, Nr. 407, Măgurele-Bucureşti, Romania*
[b] *State University of New York at Buffalo, Department of Chemistry, 410 NSC, Buffalo, NY 14260-3000, USA*
[c] *Universitatea Babeş-Bolyai, Facultatea de Chimie şi Inginerie Chimică, Str. Kogălniceanu, Nr. 1, RO-400084 Cluj-Napoca, Romania, mcotisel@chem.ubbcluj.ro*

Previously, we have reported that the local anesthetics, like procaine, expand the lipid monolayers spread at the air/water interface, at low and intermediate surface pressures, depending on the pH's, ionic strengths and surface characteristics of the chosen lipid [6-24].

The interfacial characteristics of the mixed lipid and procaine monolayers results from the adsorption on and the penetration of procaine into lipid membrane models in substantial agreement with other related published data [1-5, 22-29].

The objective of the present work is to analyse the effects of procaine on the structural and topographical characteristics of lipid monolayers using atomic force microscopy (AFM) and Langmuir-Blodgett technique (LBT). We have chosen a synthetic phospholipid, namely L-α dipalmitoyl phosphatidyl choline (1, 2-dipalmitoyl -sn- glycero-3-phospho-choline: DPPC), which forms stable monolayers at fluid interfaces [30-32]. Here, we investigate the structure and surface topography of the DPPC monolayers spread on aqueous solution in the absence and the presence of procaine and the formation of liquid condensed domains is evidenced.

RESULTS AND DISCUSSION

The surface pressure versus mean molecular area isotherms were recorded for pure DPPC monolayers, spread at the air/water (pH 5.6) interface, and for mixed DPPC and procaine monolayers, obtained by spreading DPPC monolayers on procaine (10^{-3} M) aqueous phase (pH 5.2), at 20 ^{o}C. For pure DPPC monolayer, the compression isotherm shows a phase transition at a lateral surface pressure of about 8 mN/m, from liquid expanded (LE) to liquid condensed (LC) state [30]. The mixed DPPC and procaine monolayer also presents a LE/LC phase transition, evidenced on compression isotherm, at around 15 mN/m.

In addition, the compression isotherms show a collapse phenomenon at very high surface pressures, characterized by collapse area (A_c) and collapse pressure (π_c). The collapse characteristics and the limiting molecular areas (A_0), characterizing the LC phase of DPPC monolayers, are given in Table 1.

Table 1. Surface characteristics of DPPC monolayers spread at the air/water interface both in the absence and in the presence of procaine (P) in aqueous phase.

Monolayer	P (M)	A_0 (Å^2)	A_c (Å^2)	π_c (mN/m)
DPPC	0	54	42	55
DPPC and P	10^{-3}	78	42	63

From Table 1, it is observed the expanded effect of procaine, namely the limiting molecular area (A_0) for LC state and the collapse pressure (π_c) are much higher in the presence of procaine than for pure DPPC monolayers. These data indicate that procaine has a notable effect both on the DPPC phase transition and on the collapse of DPPC monolayers, at the air/water interface. Due to the same collapse areas, (A_c), it is found that the procaine is excluded from DPPC monolayers at collapse, but still remains adsorbed on DPPC monolayer surface thus, increasing the monolayer collapse pressure and stability. This effect might correspond to pressure-driven exclusion of procaine from zwitterionic DPPC monolayers.

Similar expansion effects were previously reported for octadecanoic acid [22, 24] and for tetradecanoic acid [23] spread on procaine aqueous phase. The magnitude of the effect increased with increasing procaine concentration in the aqueous phase.

The surface topography of pure DPPC monolayers, transferred at 8 mN/m on mica surface, is given in the AFM images, Figs. 1 and 2. The 2D topographies show a heterogeneous DPPC monolayer with characteristic features and the domains formation is clearly evidenced.

Brighter areas (Figs. 1 and 2) are assigned for high domains of the DPPC in LC state, but darker areas correspond to lower domains characteristic for LE phase. The boundaries of DPPC domains are typically observed and are thought to be the borders between various DPPC areas with different tilt of molecular orientations [19, 30, 32]. We suggest that the lighter domains correspond to well organized probably almost vertically oriented DPPC molecules, while the darker areas correspond to less orderly DPPC molecules. The LC domains are distributed within the LE matrix of DPPC monolayers.

The analysis of surface topographies, Figs. 1 and 2, clearly indicate the phase separation between LC and LE phases, which is consistent with the two surface phase transition recorded at the lateral surface pressure of 8 mN/m, as it is evidenced on compression isotherms. The AFM images of DPPC monolayers show nano island LC domains (with long axis of isolated 20 nm up to 100 nm domains, Fig. 1B). The large LC domains are observed in Figs. 1A and 2 (with long axis from 500 nm up to 2 and 3 μm). Also, micro islands of LC phase are identified particularly at big scanned areas (e.g., 25 μm x 25 μm) with major axis up to 3 or even 8 μm.

The large LC domains are almost circular or elongated (Fig. 1A and Fig. 2A). The nano LC domains are predominantly circulars, square or elongated associated as asymmetric clusters, like windmill shape (Fig. 1B and 2) as previously observed by fluorescence microscopy [23], by direct compression of DPPC monolayer at the air/water interface. The large LC domains are higher with 0.8, 1.5 or 2 nm than the LE phase. It is to be noted that the large LC domains show almost the same height as the surrounding nano LC domains.

Ultimately, near the DPPC monolayer collapse a homogeneous structure results from the close packed DPPC molecules, well oriented vertically at the air/water interface, as a consequence of strong molecular interactions.

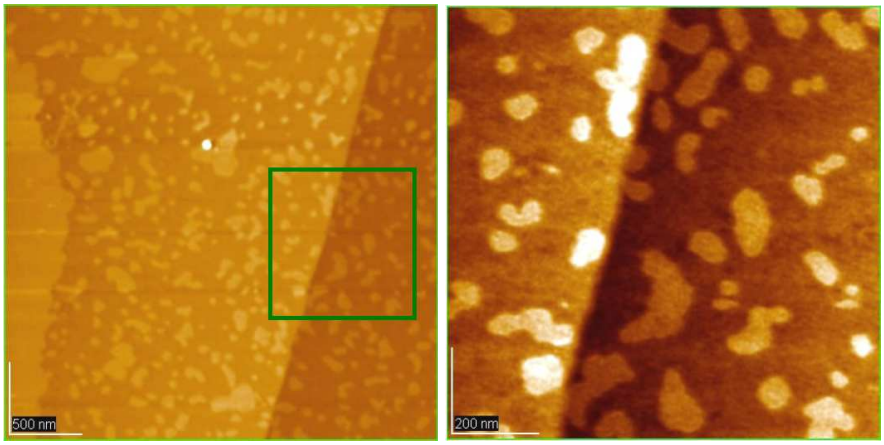

(A) (B)

Figure 1. AFM topography images of DPPC monolayers, for 3 μm x 3 μm (A) and 1 μm x 1 μm (B) scanned areas. Monolayers were transferred by Langmuir-Blodgett technique on mica surface, at 8 mN/m, for the liquid expanded (LE) to liquid condensed (LC) phase transition. The z-scale is 5 nm for image A and 3 nm for image B. Image B was recorded by scanning on small area marked in image A.

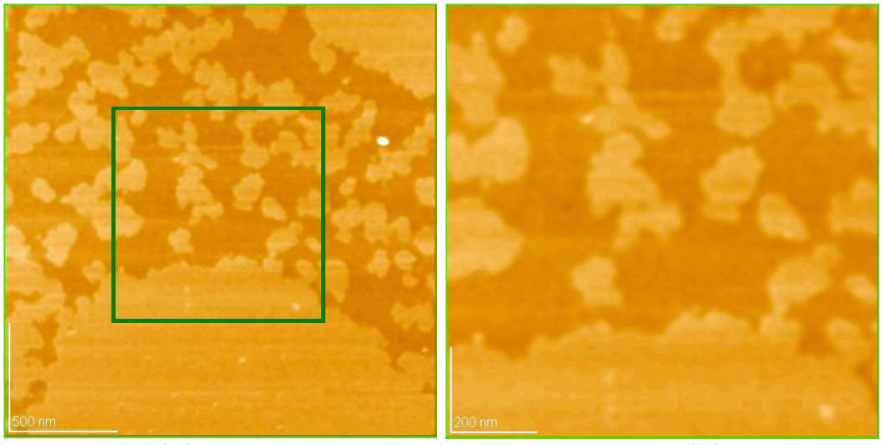

(A) (B)

Figure 2. AFM topography images of DPPC monolayers, for 2 μm x 2 μm (A) and 1 μm x 1 μm (B) scanned areas. Monolayers were transferred at the phase transition (8 mN/m) on mica surface. The z-scale is 5 nm for image A and 3 nm for image B. Image B was recorded by scanning on small area marked in image A.

The presence of procaine (0.001 M in aqueous phase, pH 5.2) causes changes in surface properties of DPPC monolayers as determined on compression isotherms and in the structure of DPPC layers as observed on AFM images.

The LE/LC phase transition is evidenced on compression isotherms for mixed DPPC and procaine monolayers, at 15 mN/m. Thus, a substantial increase in transition lateral surface pressure is recorded for mixed monolayers as compared with pure DPPC monolayers (i.e., 8 mN/m) on water.

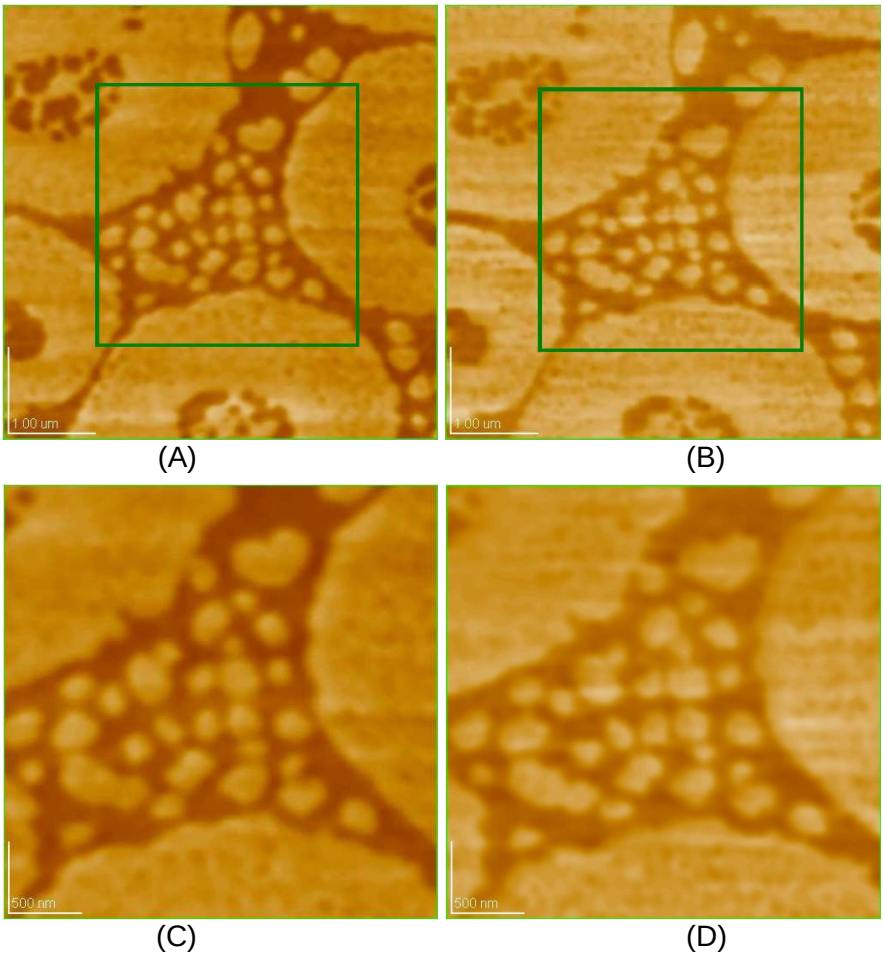

Figure 3. Topographies (A and C) and phase images (B and D) of DPPC monolayers spread on aqueous phases of 0.001 M procaine, transferred on mica at 8 mN/m. A and B: scanned area 5 µm x 5 µm; C and D: 3 µm x 3 µm. AFM images (C and D) were recorded by scanning on small areas marked in images A and B, respectively. The *z*-scale is 5 nm for A and C topographies.

For the beginning, the AFM images for mixed DPPC and procaine monolayers, transferred on mica at the lateral surface pressure of 8 mN/m, are examined (Fig. 3) and compared with AFM images of pure DPPC monolayers (Figs. 1 and 2). A phase separation is also found and visualized in AFM images for mixed DPPC and procaine monolayers (Fig. 3) in a similar way with the situation for pure DPPC monolayers (Figs 1 and 2). Thus, the LC domains within mixed DPPC and procaine monolayers are detected at low value of lateral surface pressure (about 8 mN/m). The LC domains in mixed monolayers are smaller (Fig. 3) than those observed in DPPC monolayers on a pure water substrate (Fig. 1A), at the lateral pressure of 8 mN/m, which is characteristic for the phase transition within the pure DPPC monolayers.

As the compression of mixed DPPC and procaine monolayers continued, the LC domains increased in size and number (Fig. 4, for 14 mN/m).

Furthermore, for mixed DPPC and procaine monolayers at the LE/LC phase transition (about 15 mN/m) recorded on compression isotherm, it was observed a continuous increase in the LC domains, which carry various interesting shapes. In other words, at 10^{-3} M procaine concentration, the LE/LC phase transition of mixed monolayers was observed by AFM images (Fig. 5, at the transition lateral surface pressure of about 15 mN/m), while the formation of LC phase was detected at much lower pressures, like 8 mN/m (Fig. 3) and at 14 mN/m (Fig. 4).

Clearly, procaine induces nucleation of liquid condensed domains before the phase transition recorded on compression isotherms for mixed DPPC and procaine monolayers. It appears that the onset of the LE/LC phase transition starts before the transition lateral surface pressure for mixed monolayers.

At lateral pressures above the phase transition, e.g. 20 mN/m, still some very large LC domains are visualized in AFM images. Near the collapse, the mixed DPPC and procaine monolayers are well ordered as in the case of pure DPPC monolayers showing a very low roughness (rms about 0.2 nm).

Undoubtedly, the presence of procaine in aqueous phase brings strong modifications on the structure and morphology of DPPC monolayers, even at low lateral surface pressure of 8 mN/m, which is characteristic for LE/LC phase transition of pure DPPC monolayers.

We suggest that procaine coexists with less ordered DPPC molecules and is preferentially located at the domain boundaries. This would indicate that the lighter domains correspond to almost highly oriented DPPC molecules. The dark domains probably correspond to less organized DPPC molecules mixed with procaine. Thus, AFM images reveal a phase separation between DPPC condensed phase (high areas) and DPPC expanded phase enriched in procaine (low areas).

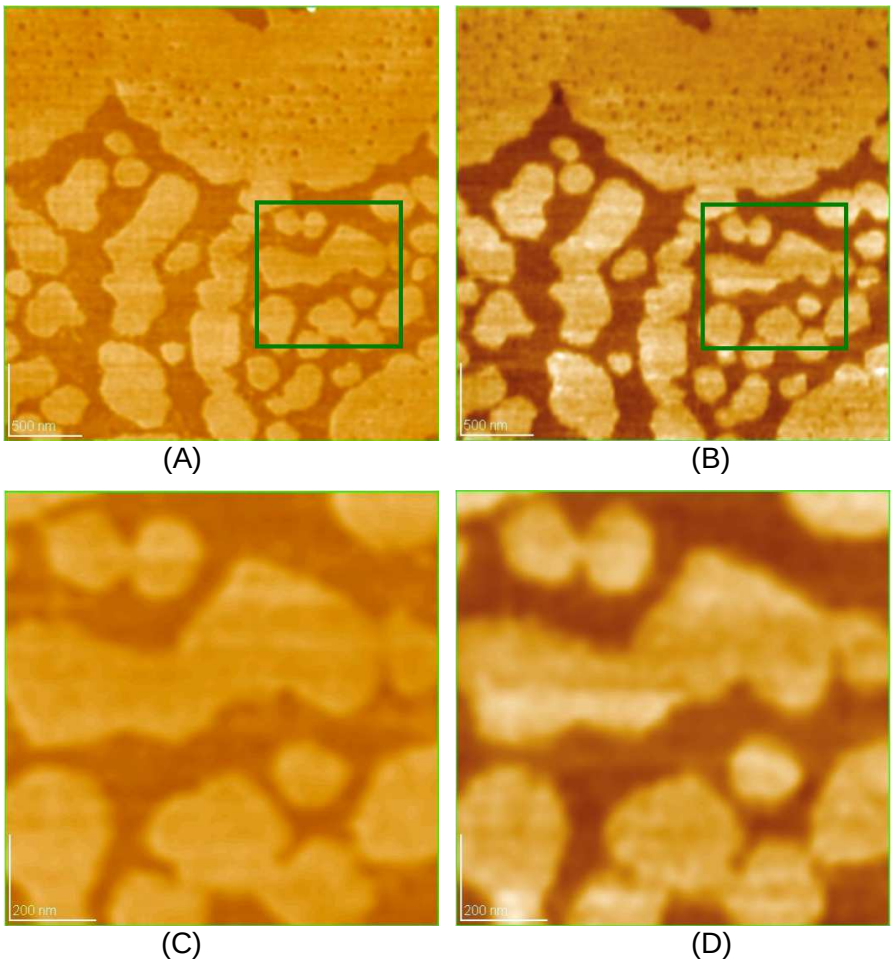

Figure 4. Topographies (A and C) and phase images (B and D) of DPPC monolayers spread on aqueous phases of 0.001 M procaine, compressed to 14 mN/m and transferred on mica surface. A and B: scanned area 3 μm x 3 μm; C and D: 1 μm x 1 μm. AFM images (C and D) were recorded by scanning on small areas marked in images A and B, respectively. The *z*-scale is 5 nm for A and C topographies.

The mixed DPPC and procaine monolayers present LC nano domains co-existing with small round LE procaine rich phase in the center of the LC large micro domains (Fig. 3A and B), where the LC nano domains form a network of filament unique structure. Also, the LC nano domains are situated at the edges of the large LC domains forming larger aggregates (Fig. 3C and D), belts (Fig. 4A and B) or stripes (Fig. 4C and D).

By increasing the surface pressure (Fig. 4, at 14 mN/m), the stripes are formed by the alignment of many smaller LC domains, that have almost the same height with the large LC domains of DPPC monolayers.

The phase images (Figs. 3B, 3D, 4B and 4D) show the morphological character more clearly than the corresponding topography (Figs. 3A, 3C, 4A and 4C) due to the difference in the surface physical and chemical properties between the condensed and expanded DPPC monolayers.

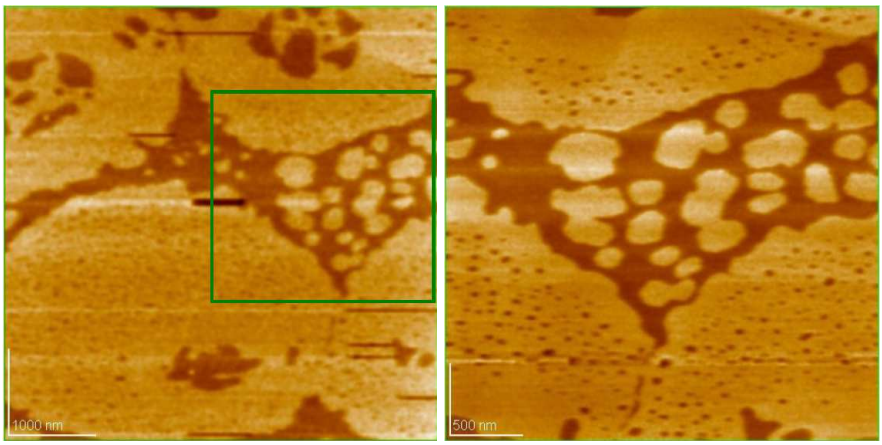

(A) (B)

Figure 5. Topographies (A and B) of DPPC monolayers spread on aqueous phases of 0.001 M procaine, compressed at about 15 mN/m and transferred on mica surface by LB technique. A: scanned area of 5 μm x 5 μm. (B): 3 μm x 3 μm were recorded by scanning on small areas marked in image A. The *z*-scale is 5 nm.

Thus, almost in the center of the large LC domains, many nano LC domains are observed (with axis of 50 to 150 nm), particularly in small scale images (Figs. 3 and 5). The large LC domains have the same height as the edges of the aligned stripes.

The large LC domains are about 2 nm higher than the fluid LE phase and are surrounded by a mixture of LE phase and LC nano domains, in which LC domains are aligned in a striped pattern (Fig. 5). The large LC domains are rather well packed at high lateral surface pressure (15 mN/m) that corresponds to the phase transition of mixed DPPC:P monolayers evidenced on compression isotherm.

Thus, a unique morphology of mixed DPPC and procaine monolayers is observed, showing large LC domains, which contain a network of filaments of LC domains surrounded by LE procaine rich phase, where the

procaine is adsorbed preferentially at the edge of the LC domains. At the transition surface pressure (15 mN/m), numerous filaments in the center of the large LC domains are formed (Fig. 5A) and larger patches at their edges appears (Fig. 5B).

The differing shapes of LC phase within the mixed DPPC and procaine monolayers reflect a different structure of DPPC monolayers under the action of procaine. These data suggest that procaine affects DPPC morphology in the LC phase. Nevertheless, the morphological changes within mixed DPPC and procaine monolayers support the participation of procaine in anesthesia.

Higher amounts of procaine in aqueous phase give numerous filaments in the center of the LC micro domains and evidently larger LC patches at their edges.

Qualitatively, the same effects were observed at lower procaine concentrations. However, the magnitude of the procaine effects was smaller and was diminished with decreasing of procaine concentrations.

This situation might be related to the fact that the procaine adsorbs and penetrates preferably at the boundaries between LC domains, with a different tilt direction, and in the expanded DPPC phase, as also found by epifluorescent microscopy [23]. However, the binding of procaine molecules to the surface of the DPPC condensed domains could also perturb the lipid chains organization. In this regard, the maximum height in mixed monolayers is about 3.6 nm as determined in Fig. 3. This height corresponds to the mixed DPPC and procaine condensed domains, and is decreased as compared to the height of the condensed domains existing in pure DPPC layers (Fig. 1A, where maximum height of 4.3 nm was found). The phase contrast images, given in Figs. 3 and 4, show also clearly the morphological character corresponding to the given surface topography.

The tertiary amine procaine is an amphiphilic molecule which exists in the charged form [13] at the working pH of about 5.6. The hydrophilic amine moiety is responsible for water solubility and DPPC membrane surface binding and the hydrophobic moiety appears to control the organization within the DPPC membrane model. The interaction of procaine molecules with zwitterionic DPPC molecules may lead to an ordering effect on the DPPC monolayer interface and to a disordering effect on the hydrocarbon interior of DPPC monolayers, in substantial agreement with AFM observations.

In order to explain the mode of action of procaine, positively charged under the working conditions, on the zwitterionic phospholipids monolayers, we assume that positively charged procaine molecules adsorb onto the lipid membrane surface. This will allow the hydrophobic portion of procaine molecule to be embedded into the hydrocarbon part of the expanded liquid phase and at the domain boundaries of lipid monolayers.

The positively charged amine group of procaine molecules can interact electrostatically, at the monolayer/water interface, with the negatively charged group of the zwitterionic DPPC molecules. The electrostatic interaction will appear in both the condensed and the expanded liquid state of DPPC monolayers increasing the stability of the lipid membrane.

The findings in this study suggest that procaine accumulates in the lipid phase of cell membranes, and thus might change the physical properties of the membrane lipid and consequently, procaine molecules influence the protein conformation. The effect of procaine and other local anesthetics on DPPC membrane structuration at various lateral surface pressures is under further investigation in our laboratories.

CONCLUSIONS

Combined surface chemistry, Langmuir-Blodgett (LB) self-assembly technique, and atomic force microscopy have been used to determine the spreading, structure and topography of DPPC monolayers at the air/water interface.

During compression at the air/water interface, DPPC monolayers present a structural transition at a lateral surface pressure of about 8 mN/m, from liquid expanded (LE) to liquid condensed (LC) structures, showing LC domains with heterogeneous structures. Finally, near the DPPC monolayer collapse a homogeneous structure results from the close packed DPPC molecules, well oriented in a matrix at the air/water interface, which is a consequence of the strong molecular interactions.

The LB self-assembled monolayers were transferred from Langmuir films onto mica, at controlled surface pressures characteristic for the phase transition in DPPC monolayers by using vertical transfer method. In the presence of procaine (10^{-3} M) in aqueous phase, the stability of DPPC films is highly increased as it is reflected by the increased collapse and phase transition pressures of DPPC monolayers.

The DPPC monolayer structure is influenced by the presence of procaine in aqueous phase and a more expanded monolayer structure is observed for 10^{-3} M procaine. AFM images confirm, at the microscopic and nanoscopic levels, almost the same type of structural changes deduced from the compression isotherms for DPPC monolayers as a function of surface pressure.

Structural characteristics and the surface topography of DPPC monolayers are highly dependent on the lateral surface pressure for a particular concentration of procaine in the aqueous phase. In addition, the appearance of a new liquid condensed (LC) phase is strongly evidenced in the mixed DPPC and procaine monolayers.

The results reveal some specific molecular interactions between DPPC and procaine in substantial agreement with molecular interactions and with molecular structure of these biocompounds.

EXPERIMENTAL SECTION

Materials

Synthetic 1,2-dipalmitoyl-*sn*-glycero-3-phosphocholine: DPPC, and procaine, 2-(diethylamine)ethyl-*para*-(amine) benzoate, hydrochloride (P- HCl), were purchased from Sigma Chemical Co., and used without further purification. For the study of the procaine effect, P- HCl was first dissolved in two-distilled water, giving a chosen procaine concentration, e.g., 10^{-3} M procaine, in the aqueous solution.

Langmuir-Blodgett (LB) film

DPPC was dissolved in a mixture of chloroform: ethanol (9:1, v/v), giving a 1 mM phospholipid in organic solution. The DPPC solution was spread at the air/water interface with a microsyringe both in the absence and the presence of procaine in aqueous solutions. After spreading, the system was allowed to stand for 10 min, without causing the surface disturbance. Then, the compression isotherms in terms of surface pressure versus mean molecular area of DPPC were recorded. All measurements were performed with KSV equipment. The speed of the compression was 10 mm min^{-1} (i.e., 8 $Å^2$/(molecule x min). For AFM observations, a single layer (LB film) was transferred on freshly cleaved mica surface, using a vertical dipping method at different surface pressures maintained constant (e.g., 8 mN/m). The LB film transfer took place at a rate of about 5 mm/min.

AFM observations

Atomic force microscopy (AFM) is a surface imaging technique with a nanometer-scale resolution [32-35]. AFM studies were performed using the AFM JEOL 4210. The cantilevers with a resonance frequency of 250 – 350 kHz were used. Triplicate samples were prepared for each monolayer composition and at least four separate areas were imaged for each sample. Through this study, AFM images were obtained at several constant surface pressures in order to examine the effect of procaine on the phase behaviour of DPPC monolayers spread at the air/water interface.

REFERENCES

1. H. Tsuchiya, M. Mizogami, T. Ueno, K. Takakura, *Inflammopharmacol*., **2007**, *15*, 164.
2. T. Hata, H. Matsuki, S. Kaneshina, *Colloids Surf. B*, **2000**, *18*, 41.
3. Z. Leonenko, E. Finot, D. Cramb, *Biochim. Biophys. Acta,* **2006**, *1758*, 487.
4. H. Matsuki, S. Kaneshina, H. Kamaya, I. Ueda, J. *Phys. Chem. B,* **1998**, *102*, 3295.

5. Z. V. Leonenko, D. T. Cramb, *Can. J. Chem.,* **2004**, *82*, 1128.
6. M. Tomoaia-Cotisel, E. Chifu, A. Mocanu, J. Zsakó, M. Salajan, P.T. Frangopol, *Rev. Rroum. Biochim.,* **1988**, *25**(** 3)*, 227.
7. M. Tomoaia-Cotisel, J. Zsakó, E. Chifu, P. T. Frangopol, W. A. P. Luck, E. Osawa, *Rev. roum. Biochim.,* **1989**, *26**(**4)*, 305.
8. J. Zsakó, M. Tomoaia-Cotisel, E. Chifu, A. Mocanu, P. T. Frangopol, *Biochim. Biophys. Acta,* **1990**, *1024*, 227.
9. J. Zsakó, M. Tomoaia-Cotisel, E. Chifu, I. Albu, A. Mocanu, P. T. Frangopol, *Rev. Roum. Chim.,* **1990**, *35(7-9)*, 867.
10. E. Chifu, M. Tomoaia-Cotisel, J. Zsakó, I. Albu, A. Mocanu, P.T. Frangopol, *Rev. Roum. Chim.,* **1990**, *35(7-9)*, 879.
11. M. Tomoaia-Cotisel, E. Chifu, S. Jitian, I. Bratu, S. Bran, P. T. Frangopol, A. Mocanu, *Stud. Univ. Babes-Bolyai, Chem.,* **1990**, *35(2)*, 17.
12. E. Chifu, M. Tomoaia-Cotisel, J. Zsakó, A. Mocanu, M. Salajan, M. Neag, P. T. Frangopol, *Seminars in Biophysics, Vol. 6***,** Editors: P. T. Frangopol, V. V. Morariu, IAP Press, Bucharest, **1990**, 117.
13. J. Zsakó, M. Tomoaia-Cotisel, I. Albu, A. Mocanu, E. Chifu, P. T. Frangopol, *Rev. roum. Biochim.,* **1991**, *28(1-2)*, 33.
14. M. Tomoaia-Cotisel, E. Chifu, J. Zsakó, P. T. Frangopol, P. J. Quinn, A. Mocanu, *Stud. Univ. Babes-Bolyai, Chem.,* **1993**, *38(1-2)*, 81.
15. J. Zsakó, M. Tomoaia-Cotisel, E. Chifu, A. Mocanu, P. T. Frangopol, *Gazz. Chim. Ital.,* **1994**, *124*, 5.
16. J. Zsakó, E. Chifu, M. Tomoaia-Cotisel, A. Mocanu, P. T. Frangopol, *Rev. Roum. Chim.,* **1994**, *37(7)*, 777.
17. M. Tomoaia-Cotisel, J. Zsakó, E. Chifu, A. Mocanu, P. T. Frangopol, P. J. Quinn, *J. Romanian Colloid and Surface Chem. Assoc.,* **1997**, *2(3-4)*, 30.
18. M. Tomoaia-Cotisel, T. Oproiu, J. Zsako, A. Mocanu, P. T. Frangopol, P. J. Quinn, *Rev. Roum. Chim.,* **2000**, *45(9)*, 851.
19. M. Tomoaia-Cotisel, A. Mocanu, *Rev. Chim. (Bucharest),* **2008,** *59(11)*, 1230.
20. P. T. Frangopol, D. Mihailescu, *Colloids Surf. B,* **2001**, *22*, 3.
21. T. Hianik, M. Fajkus, B. Tarus, P. T. Frangopol, V. S. Markin, D. F. Landers, *Bioelectrochem. Bioenergetics,* **1998**, *46*, 1.
22. M. Tomoaia-Cotisel, D. A. Cadenhead, *Langmuir,* **1991**, *7*, 964.
23. B. Asgharian, D. A. Cadenhead, M. Tomoaia-Cotisel, *Langmuir,* **1993**, *9*, 228.
24. M. Tomoaia-Cotisel, *Progr. Colloid Polym. Sci.,* **1990**, *83*, 155.
25. H. Matsuki, K. Shimada, S. Kaneshina, M. Yamanaka, H. Kamaya, I. Ueda, *Langmuir,* **1997**, *13*, 6115.
26. S.-Y. Choi, S.-G. Oh, J.-S. Lee, *Colloids Surf. B,* **2001**, 20, 239.
27. A. Cavalli, G. Borissevitch, M. Tabak, O. N. Oliveira, Jr., *Thin Solid Films,* **1996**, *284*, 731.
28. D. M. Goodman, E. M. Nemoto, R. W. Evans, P. M. Winter, *Chemistry and Physics of Lipids,* **1996**, *84*, 57.
29. S.-Y. Choi, S.-G. Oh, J.-S. Lee, *Colloids Surf. B,* **2000**, *17*, 255.
30. M. Tomoaia-Cotisel, J. Zsako, E. Chifu, *Ann. Chim. (Rome),* **1981**, *71(3)*, 189.
31. G. Chimote, R. Banerjee, *Colloids Surf. B,* **2008**, *65*, 120.
32. S. Yokoyama, Y. Ohta, H. Sakai, M. Abe, *Colloids Surf. B,* **2004**, *34*, 65.

33. M. Tomoaia-Cotisel, Convergence of Micro-Nano-Biotechnologies, Series in Micro and Nanoengineering, Vol. *9,* Editors: M. Zaharescu, E. Burzo, L. Dumitru, I. Kleps, D. Dascalu, Romanian Academy Press, Bucharest, **2006**, 147.
34. K. Hoda, Y. Ikeda, H. Kawasaki, K. Yamada, R. Higuchi, O. Shibata, *Colloids Surf*. B, **2006**, *52*, 57.
35. Gh. Tomoaia, M.Tomoaia-Cotisel, A. Mocanu, O. Horovitz, L.-D. Bobos, M. Crisan, I. Petean, *J. Optoelectron. Adv. Materials*, **2008**, *10(4)*, 961.